Stem Cell Research 60 (2022) 102677

Contents lists available at ScienceDirect

Stem Cell Research

journal homepage: www.elsevier.com/locate/scr

Lab Resource: Genetically-Modified Multiple Cell Lines

Generation of homozygous $Na_v1.8$ knock-out iPSC lines by CRISPR Cas9 genome editing to investigate a potential new antiarrhythmic strategy

Wiebke Maurer [a], Nico Hartmann [a], Loukas Argyriou [b], Samuel Sossalla [a,c], Katrin Streckfuss-Bömeke [a,d,*]

[a] Clinic for Cardiology and Pneumology, Georg-August University Göttingen, and DZHK (German Center of Cardiovascular Research), Partner Site Göttingen, Göttingen, Germany
[b] Institute of Human Genetics, University Medical Center Göttingen (UMG), and DZHK (German Center of Cardiovascular Research), Partner Site Göttingen, Germany
[c] Department of Internal Medicine II, University Medical Center Regensburg, Regensburg, Germany
[d] Institute of Pharmacology and Toxicology, University of Würzburg, Würzburg, Germany

A B S T R A C T

The sodium channel $Na_v1.8$, encoded by *SCN10A*, is reported to contribute to arrhythmogenesis by inducing the late I_{Na} and thereby enhanced persistent Na^+ current. However, its exact electrophysiological role in cardiomyocytes remains unclear. Here, we generated induced pluripotent stem cells (iPSCs) with a homozygous *SCN10A* knock-out from a healthy iPSC line by CRISPR Cas9 genome editing. The edited iPSCs maintained full pluripotency, genomic integrity, and spontaneous *in vitro* differentiation capacity. The iPSCs are able to differentiate into iPSC-cardiomyocytes, hence making it possible to investigate the role of $Na_v1.8$ in the heart.

1. Resource Table

Unique stem cell line identifier	UMGi158-A UMGi158-A-1
Alternative name(s) of stem cell line	Nav1.8_KO_K62.1 Nav1.8_KO_K62.4
Institution	Clinic for Cardiology and Pneumology, University Medical Center Göttingen
Contact information of the reported cell line distributor	Katrin Streckfuss-Bömeke; katrin.streckfuss@med.uni-goettingen.de; katrin.streckfuss-boemeke@uni-wuerzburg.de
Type of cell line	Human induced pluripotent stem cell (hiPSC)
Origin	Human
Additional origin info *(applicable for human ESC or iPSC)*	Age: 25 years Sex: female Ethnicity: Caucasian
Cell Source	Skin fibroblasts
Method of reprogramming	N/A
Clonality	Clonal
Evidence of the reprogramming transgene loss (including genomic copy if applicable)	N/A
Cell culture system used	Feeder-free condition (Geltrex)
Type of Genetic Modification	Induced gene knock-out in healthy iPSC
Associated disease	N/A
Gene/locus	*SCN10A*/3p22.2

(*continued on next column*)

(*continued*)

Method of modification/site-specific nuclease used	Site-specific nuclease (SSN) CRISPR/Cas9
Site-specific nuclease (SSN) delivery method	RNP electroporation
All genetic material introduced into the cells	Cas9, gRNA1, gRNA2, tracrRNA
Analysis of the nuclease-targeted allele status	Sequencing of the targeted allele
Method of the off-target nuclease activity surveillance	Sanger sequencing
Name of transgene	N/A
Eukaryotic selective agent resistance (including inducible/gene expressing cell-specific)	N/A
Inducible/constitutive system details	N/A
Date archived/stock date	23.10.2019
Cell line repository/bank	https://hpscreg.eu/cell-line/UMGi158-Ahttps://hpscreg.eu/cell-line/UMGi158-A-1
Ethical/GMO work approvals	Ethical committee of University Medical Center Göttingen (Az-10/9/15)
Addgene/public access repository recombinant DNA sources' disclaimers (if applicable)	N/A

* Corresponding author at: Institute of Pharmacology and Toxicology, University of Würzburg, Versbacher Str. 9, Würzburg D- 97078, Germany.
E-mail address: katrin.streckfuss-boemeke@uni-wuerzburg.de (K. Streckfuss-Bömeke).

https://doi.org/10.1016/j.scr.2022.102677
Received 20 November 2021; Received in revised form 7 December 2021; Accepted 17 January 2022
Available online 19 January 2022

2. Manuscript section expected contents clarification

2.1. Resource utility

The sodium channel $Na_v1.8$ (encoded by the *SCN10A* gene) is slightly expressed in cardiomyocytes, however its exact role is not clear so far. To unravel the role of $Na_v1.8$ exactly and to clearly distinguish its role from other sodium channels a homozygous *SCN10A* knock-out iPSC line was generated. Table 1

2.2. Resource details

In heart failure (HF), enhanced persistent Na^+ current (late I_{Na}) exerts detrimental effects on cellular electrophysiology and can induce arrhythmias. We have shown that the expression of the non-cardiac Na^+ channel $Na_v1.8$ is upregulated in human failing myocardium, and that $Na_v1.8$ contributes to arrhythmogenesis by inducing the late I_{Na} (Dybkova et al., 2018; Ahmad et al., 2019). In addition, genome wide association studies reported that variants in the *SCN10A* gene ($Na_v1.8$) are associated with cardiac arrhythmias such as atrial fibrillation and sudden death (Jabbari et al., 2015). However, it is still controversially discussed whether these $Na_v1.8$-related effects are mediated by cardiac ganglia or cardiomyocytes. To study the electrophysiological contribution of $Na_v1.8$ in iPSC-cardiomyocytes, a homozygous *SCN10A* knock-out iPSC line was generated by CRISPR Cas9 genome editing from a previously described healthy iPSC line, reprogrammed from skin fibroblasts by using a non-integrating plasmid system (Borchert, 2017). The knock-out (KO) lines were generated using two different guideRNAs, both targeting *SCN10A* exon1 by aiming spontaneous insertion/deletion events leading to frameshifts and premature stop codons (Fig. 1A). Two identical clones (K62.1, K62.4) were generated harboring identical frameshifts leading to premature stop codons on both alleles (Fig. 1B, Supplementary Fig. 1). Both clones originated from an edited/wildtype mixed clone (K62) after additional singularization. These mutations were preserved over several passages and were checked frequently by Sanger sequencing using a primer pair directed against exon1 (Table 2). The top four predicted off-targets of each gRNA were analyzed by Sanger sequencing (Supplemenatry Fig. 2). Control lines were used for comparison. The analyzed sequences showed no editing event (Supplemenatry Fig. 2). Genomic integrity was analyzed by G-banding and both KO iPSC lines harbor a normal karyotype (Fig. 1C). Both KO lines maintained full pluripotency characteristics as shown in Fig. 1. QPCR analysis demonstrated the significantly increased expression of pluripotency markers like *OCT4, SOX2, NANOG* and *LIN28* in both KO lines in comparison to fibroblasts as a negative control (NC) and comparable expression to the iPSC line, from which they derived as a positive control (PC) (Fig. 1D). Additionally, they showed classical iPSC morphology, expression of alkaline phosphatase (ALP) and were positive for staining of classical pluripotency markers on protein level, such as OCT4, SOX2, LIN28 and TRA1-60 (Fig. 1E). The KO iPSC lines were authenticated by STR analysis and matched with the healthy iPSC line, from which they derived.

Spontaneous differentiation capacity was analysed by *in vitro* embryoid body formation. The expression of markers of all three germ layers were tested on protein level by immunofluorescence staining of α-smooth muscle actin (α-SMA) (Mesoderm), α-fetoprotein (AFP) (Endoderm), and β-III-Tubulin (Ectoderm) (Fig. 1F). Expression of germ layer marker was also confirmed on mRNA level by semi-quantitative PCR for *AFP, ALB, cTNT, αMHC, MAP2* and *PAX6* (Fig. 1F). *OCT4* expression in contrast is decreased during differentiation. The iPSCs are able differentiate into ventricular iPSC-cardiomyocytes as shown by *MLC2v* expression (Fig. 1G).

Using the homozygous Nav1.8 knock out iPSC-lines described here, we previously demonstrated that $Na_v1.8$ contributes to INa_L formation (Bengel et al., 2021).

Table 1
Characterization and validation.

Classification (optional *italicized*)	Test	Result	Data
Morphology	Light microscopy and photography	Brightfield images show normal stem cell-like morphology	Fig. 1 panel E
Pluripotency status evidence for the described cell line	Qualitative analysis of immunofluorescence stainings	Positive immunostainings of pluripotency markers OCT4, SOX2, LIN28, TRA1-60	Fig. 1 panel E
	Quantitative analysis (RT-qPCR)	iPS cells of Nav1.8 KO clones show comparative expression pattern of *OCT4, NANOG, SOX2, LIN28* compared to the already published healthy iPSC line. Skin fibroblasts (NC) show low expression of corresponding genes.	Fig. 1 panel D
Karyotype	Karyotype (G-banding) and resolution	46XX, Resolution 300	Fig. 1 panel C
Genotyping for the desired genomic alteration/allelic status of the gene of interest	PCR across the edited site + Sanger sequencing	The edited iPSC line is a homozygous knock-out line, where both alleles showed different insertions and deletions, both leading to premature stop codons.	Fig. 1 panel B Supplementary Fig. 1
	Transgene-specific PCR	N/A	N/A
Verification of the absence of random plasmid integration events	PCR/Southern	N/A	N/A
Parental and modified cell line genetic identity evidence	STR analysis	16 independent loci (amelogenin, D8S1179, D21S11, D7S820, CSF1PO, D3S1358, TH01, D13S317, D16S539, D2S1338, vWA, TPOX, D18S51, D5S818, FGA) were analyzedand matched	submitted in the archive with journal
Mutagenesis / genetic modification outcome analysis	Sequencing (genomic DNA PCR product)	Sequencing of the PCR band showed a Cytosin deletion and CAC insertion in Exon1 on allele1 and a CT deletion in Exon1 on allele2. Both variations lead to premature stop codons in Exon1, while the sequencing of the parental line did show the wildtype sequence only.	Fig. 1 panel B Supplementary Fig. 1
	PCR-based analyses	N/A	N/A
		N/A	N/A

(*continued on next page*)

Table 1 (*continued*)

Classification (optional *italicized*)	Test	Result	Data
	Southern Blot or WGS; western blotting (for knock-outs, KOs)		
Off-target nuclease analysis-	PCR across top 5/10 predicted top likely off-target sites	Demonstration of the lack of NHEJ-caused mutagenesis in the top predicted off-target Cas nuclease activity For gRNA1 (ADORA3, CACNA2D4, KCTN1, MDH2) and for gRNA2 (CRB2, SCG5, SCL39A11, SNCA)	Sanger sequencing tracks in the Supplementary Fig. 2
Specific pathogen-free status	Mycoplasma	Negative Mycoplasma testing by luminescence	Supplementary Fig. 3
Multilineage differentiation potential	Embryoid body formation	Both clones differentiate in all three germlayers as shown by protein expression of αSMA, ßIII-tubulin and AFP and by mRNA expression of *ALB, AFP, cTNT, αMHC, PAX6, MAP2.*	Fig. 1 panel F
Donor screening (OPTIONAL)	HIV 1 + 2 Hepatitis B, Hepatitis C	N/A	N/A
Genotype - additional histocompatibility info (OPTIONAL)	Blood group genotyping	N/A	N/A
	HLA tissue typing	N/A	N/A

3. Materials and methods

3.1. Gene editing

For gene editing a previously described wildtype iPSC line (Borchert, 2017) was used. Guide RNAs (gRNA1, gRNA2) used for gene knock-out were designed to target exon1 in the *SCN10A* gene using the IDTdna.com design tool. The gRNA1: GTGACTCCGGAGTAAAGCGA*CGG* and gRNA2: ACGGAAGTTGTTAGTTTCG*AGG* were used. $2x10^6$ iPSCs were electroporated with 2.5 µl gRNA1/gRNA2 (100 µM), 5 µl tracrRNA (100 µM), 2 µl Cas9 protein (10 ng/µl, IDT) and 1 µl electroporation enhancer (100 µM, IDT) with the Human Stem Cell Nucleofector Kit (Amaxa VPH-5022) and the Amaxa Nucleofection II Device (Lonza, program B-016). 72 colonies were expanded and analysed on genomic DNA level by Sanger sequencing for successful gene editing. Two iPSC clones with homozygous *SCN10A* knock-out were chosen after additional singularization of an edited/wildtype mixed clone.

3.2. Cell culture and cardiac differentiation

The iPSCs were cultured in Essential (E8) medium (Thermo Fisher Scientific) on Geltrex®-coated 6-well dishes under humidified conditions at 37 °C and 5 % CO2 saturation. Medium was changed daily and cells were passaged when 80–90 % confluency was reached as published previously (Borchert, 2017). The cardiac differentiation was performed using manipulation of Wnt-signaling as described earlier (Borchert, 2017).

3.3. Genotyping and sequence analysis

The QIAamp® DNA Mini Kit was used for DNA isolation of iPSC clones. PCR products were extracted using the QIAquick® Gel Extraction Kit and Sanger-sequenced at Seqlab Göttingen. Primers are listed in Table 2.

3.4. In vitro spontaneous differentiation

IPSCs were cocultured with mitotically inactivated mouse embryonic fibroblasts in E8 medium in u-bottom shaped, uncoated 96-well plates for embryoid body (EB) formation. After 24 h, medium was changed to differentiation medium (Iscove's basal medium, 20 % FCS, 1x NEAA and 450 µmol/L monothioglycerol). At day 8, EBs were replated onto 12-well plates and cultured for further 10 or 25 days in differentiation medium until being analysed.

3.5. Semi-quantitative and quantitative polymerase chain reaction

RNA was isolated using the SV Total RNA Isolation System (Promega) following manufacturer's instructions. cDNA Synthesis was performed using the QuantiNova Reverse Transcription kit (Qiagen). Semi-quantitative PCR was performed using the GoTaq2 (Promega) polymerase and was analysed by 2.5 % agarose gel electrophoresis. Quantitative PCR was performed by use of the SYBR Green Mastermix (BioRad) and the CFX Connect™ Real-Time System (BioRad).

3.6. Immunofluorescence staining

IPSCs were fixed at room temperature for 20 min with 4 % Histofix (Roth) and blocked with 1 % BSA overnight. Primary antibodies were incubated overnight at 4 °C. Secondary antibody staining was performed for 1 h at 37 °C. Nuclei were visualized with 4.6-diamino-2-phenylindole (DAPI, 0.2 ng/mL). Images were taken with fluorescence microscope (Axiovert 200, Zeiss) and the Axiovision software.

3.7. Mycoplasma detection

Mycoplasma contamination tests were performed regularly with the Mycoalert Plus-Kit (Lonza) following manufacturer's instructions.

3.8. Karyotyping

GTG-Banding (Gibco® Trypsin 1:250), ThermoFisher Scientific) of 8 metaphase spreads were analysed and karyotyped using MetaClient2.0.1 software (MetaSystems) on an Axio Imager Z2 microscope (Zeiss).

3.9. STR analysis

STR analysis was performed by Eurofins Genomics.

3.10. Off-target analysis

Mismatch-based off-target prediction was conducted for all gRNAs using "Off-Spotter" (https//https://doi.org/10.1186/s13062-015-0035-

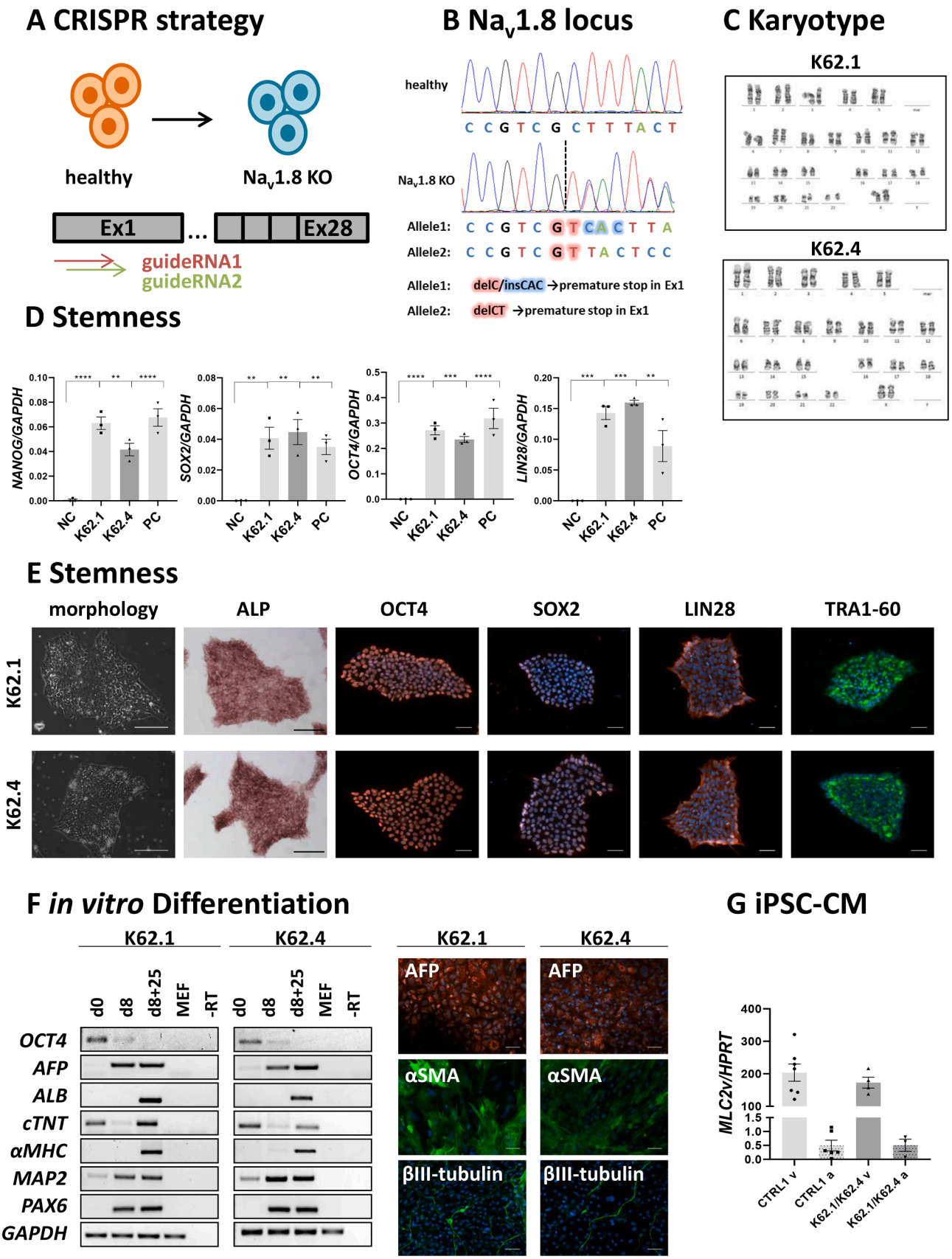
A CRISPR strategy
healthy
Nav1.8 KO
Ex1
Ex28
guideRNA1
guideRNA2
B Nav1.8 locus
healthy
C C G T C G C T T T A C T
Nav1.8 KO
Allele1: C C G T C G T C A C T T A
Allele2: C C G T C G T T A C T C C
Allele1: delC/insCAC →premature stop in Ex1
Allele2: delCT →premature stop in Ex1
C Karyotype
K62.1
K62.4
D Stemness
NANOG/GAPDH
SOX2/GAPDH
OCT4/GAPDH
LIN28/GAPDH
NC
K62.1
K62.4
PC
E Stemness
morphology
ALP
OCT4
SOX2
LIN28
TRA1-60
K62.1
K62.4
F in vitro Differentiation
K62.1
K62.4
d0
d8
d8+25
MEF
-RT
OCT4
AFP
ALB
cTNT
αMHC
MAP2
PAX6
GAPDH
AFP
αSMA
βIII-tubulin
G iPSC-CM
MLC2v/HPRT
CTRL1 v
CTRL1 a
K62.1/K62.4 v
K62.1/K62.4 a

Fig. 1.

Table 2
Reagents details.

Antibodies and stains used for immunocytochemistry/flow-cytometry			
	Antibody	Dilution	Company Cat # and RRID
Pluripotency Marker	Goat anti-OCT3/4 IgG	1:40	R&D, Minneapolis, Minnesota, USA, Cat# AF1759, RRID:AB_354975
Pluripotency Marker	Mouse anti-SOX2 IgG2a	1:50	R&D, Minneapolis, Minnesota, USA, Cat# MAB2018, RRID:AB_358009
Pluripotency Marker	Goat anti-LIN28 IgG	1:300	R&D, Minneapolis, Minnesota, USA, Cat# AF3757, RRID:AB_2234537
Pluripotency Marker	Mouse anti-TRA1-60 IgM	1:200	Abcam, Cambridge, United Kingdom, Cat# ab16288, RRID:AB_778563
Germlayer Marker	Rabbit anti-AFP IgG	1:100	Dako, Hamburg, Germany, Cat# A0008, RRID: AB_2650473
Germlayer Marker	Mouse anti-α-SMA IgG2a	1:3000	Sigma Aldrich, St. Louis, Missouri, USA, Cat# A2547, RRID:AB_476701
Germlayer Marker	Mouse anti-β-III-Tubulin	1:1000	BioLegend, San Diego, California, USA, Cat# MMS-435P, RRID:AB_2313773
Secondary antibody	Cy3 goat-anti-mouse IgG + IgM	1:300	Jackson ImmunoResearch, Cambridge, UK, Cat# 111–165-045, RRID:AB_2338003
Secondary antibody	Alexa Fluor 555 donkey-anti-goat IgG	1:1000	Thermo Fisher Scientific, Waltham, Massachusetts, USA, Cat# A-21432, RRID: AB_2535853
Secondary antibody	Alexa Fluor 488 donkey-anti-mouse IgG	1:1000	Thermo Fisher Scientific, Waltham, Massachusetts, USA, Cat# A-21202, RRID: AB_141607
Secondary antibody	Alexa Fluor 488 goat-anti-mouse IgG + IgM	1:500	Thermo Fisher Scientific, Waltham, Massachusetts, USA, Cat# A-10680, RRID: AB_2534062
Site-specific nuclease			
Nuclease information	S.p. Cas9 Nuclease V3	Integrated DNA Technologies (IDT) Cat# 1,081,058	
Delivery method	Electroporation	Amaxa Nucleofection II Device (Lonza, program B-016)	
Selection/enrichment strategy	N/A	N/A	
Primers and Oligonucleotides used in this study			
	Target	Forward/Reverse primer (5′-3′)	
Pluripotency Marker (quantitative PCR)	*SOX2*	GCTACAGCATGATGCAGGACCA/ TCTGCGAGCTGGTCATGGAGTT	
Pluripotency Marker (quantitative PCR)	*LIN28*	AGTAAGCTGCACATGGAAGG/ATTGTGGCTCAATTCTGTGC	
Pluripotency Marker (quantitative PCR)	*NANOG*	AGTCCCAAAGGCAAACAACCCACTTC/ATCTGCTGGAGG CTGAGGTATTTCTGTCTC	
Pluripotency Marker (quantitative/semi-quantitative PCR)	*OCT4*	GACAACAATGAAAATCTTCAGGAGA/ TTCTGGCGCCGGTTACAGAACCA	
House-Keeping Gene (quantitative PCR)	*GAPDH*	GTCTCCTCTGACTTCAACAGCG/ ACCACCCTGTTGCTGTAGCCA	
Germ layer marker (semi-quantitative PCR)	*AFP*	ACTCCAGTAAACCCTGGTGTTG/ GAAATCTGCAATGACAGCCTCA	
Germ layer marker (semi-quantitative PCR)	*cTNT*	GACAGAGCGGAAAAGTGGGA/ TGAAGGAGGCCAGGCTCTAT	
Germ layer marker (semi-quantitative PCR)	*ALB*	CCTTTGGCACAATGAAGTGGGTAACC/ CAGCAGTCAGCCATTTCACCATAGG	
Germ layer marker (semi-quantitative PCR)	*α-MHC*	GTCATTGCTGAAACCGAGAATG/ GCAAAGTACTGGATGACACGCT	
Germ layer marker (semi-quantitative PCR)	*MAP2*	CCACCTAGAATTAAGGATCA/GGCTTACTTTGCTTCTCTGA	
Germ layer marker (semi-quantitative PCR)	*PAX6*	CCGAGAAAGACTAGCAGCCAA/ GTGTTTGTGAGGGCTGTGTC	
House-Keeping Gene (semi-quantitative PCR)	*GAPDH*	AGAGGCAGGGATGATGTTCT/TCTGCTGATGCCCCCATGTT	
Cardiac marker (quantitative PCR)	*MLC2v*	GGCGAGTGAACGTGAAAAAT/CAGCATTTCCCGAACGTAAT	
House-Keeping Gene (quantitative PCR)	*HPRT*	CAAAGATGGTCAAGGTCGC/CAAATCCAACAAAGTCTGGCT	
Targeted mutation analysis/sequencing	*SCN10A Exon1, gDNA*	GCAAGCTGTCACCTCTCTGT/GGTGTGTGCTGTAGAACGGA	
Potential random integration-detecting PCRs	N/A	N/A	
gRNA oligonucleotide/crRNA sequence	Exon1 SCN10A	gRNA1: GTGACTCCGGAGTAAAGCGA gRNA2: GACGGAAGTTGTTAGTTTCG	
Genomic target sequence(s)	SCN10A exon 1	**CCT**CGAAACTAACAACTT**CCG**TCGCTTTACTCCGGAGTCAC (PAM site bold)	
Top off-target mutagenesis predicted site sequencing	*ADORA3*	CTAAATGTCGGCCCCTGCTT/TAGCCAGGTCCTACCTCTGC	
	CACNA2D4	TGTGTGGAAGCCGCTAGTTA/ CAGCCGTGTATACTCTCAGCC	
	KCTN1	CTCAGACCAGCAGCCTCAAA/ AGATGACACAGAGCAGGACG	
	MDH2	CTTGAGCTCGGCTTGGTTTG/AAACTCTGTGACCCCCACAC	
	CRB2	TCCCCCAAGACAGATACCCC/CAGACAGCTCATCCACCTCC	
	SCG5	GAGCTCTGAGAGGACAGCAA/ GGATTGCTCAACTGTGCTGTG	
	SLC39A11	GTTCCCCCACTGAGTCAGAA/GAAAGGGCACCGCAGTCTA	
	SNCA		

(*continued on next page*)

Table 2 (*continued*)

Antibodies and stains used for immunocytochemistry/flow-cytometry		
Antibody	Dilution	Company Cat # and RRID
ODNs/plasmids/RNA templates used as templates for HDR-mediated site-directed mutagenesis. Backbone modifications in utilized ODNS have to be noted using standard nomenclature.	TTTGGAGGAGGTGATATGCTGTA/ AAGCCTCTAGTTCTCTCTGGATTT N/A	N/A

z). The top 4 predicted off-target sites (4 mismatches compared to on-target sequence) were selected per gRNA for examination of unintended edits. Off-target site primers are listed in Table 2.

Declaration of Competing Interest

The authors declare that they have no known competing financial interests or personal relationships that could have appeared to influence the work reported in this paper.

Acknowledgments

The authors thank Johanna Heine, Yvonne Metz (Clinic for Cardiology and Pneumology, UMG) and Ilona Eggert (Institute for Human Genetics, UMG) for superb technical support. This work was supported by the Else-Kröner-Fresenius Stiftung (N.H.) and the Deutsche Forschungsgemeinschaft (DFG) through the International Research Training Group Award (IRTG) 1816 (to K.S.B.; W.M. is a fellow under IRTG 1816).

Appendix A. Supplementary data

Supplementary data to this article can be found online at https://doi.org/10.1016/j.scr.2022.102677.

References

Dybkova, N., et al., *Differential regulation of sodium channels as a novel proarrhythmic mechanism in the human failing heart.* Cardiovasc Res, 2018. **114**(13): p. 1728-1737.

Ahmad, S., Tirilomis, P., Pabel, S., Dybkova, N., Hartmann, N., Molina, C.E., Tirilomis, T., Kutschka, I., Frey, N., Maier, L.S., Hasenfuss, G., Streckfuss-Bömeke, K., Sossalla, S., 2019. *The functional consequences of sodium channel NaV 1.8 in human left ventricular hypertrophy.* ESC. Heart Fail 6 (1), 154–163.

Jabbari, J., Olesen, M.S., Yuan, L., Nielsen, J.B., Liang, B.o., Macri, V., Christophersen, I. E., Nielsen, N., Sajadieh, A., Ellinor, P.T., Grunnet, M., Haunsø, S., Holst, A.G., Svendsen, J.H., Jespersen, T., 2015. Common and rare variants in SCN10A modulate the risk of atrial fibrillation. Circ Cardiovasc Genet 8 (1), 64–73.

Bengel, P., Dybkova, N., Tirilomis, P., Ahmad, S., Hartmann, N., A. Mohamed, B., Krekeler, M.C., Maurer, W., Pabel, S., Trum, M., Mustroph, J., Gummert, J., Milting, H., Wagner, S., Ljubojevic-Holzer, S., Toischer, K., Maier, L.S., Hasenfuss, G., Streckfuss-Bömeke, K., Sossalla, S., 2021. Detrimental proarrhythmogenic interaction of Ca 2+/calmodulin-dependent protein kinase II and Na V 1.8 in heart failure. Nat Commun. 12 (1) https://doi.org/10.1038/s41467-021-26690-1.

Borchert, T., et al., 2017. Catecholamine-Dependent beta-Adrenergic Signaling in a Pluripotent Stem Cell Model of Takotsubo Cardiomyopathy. J Am Coll Cardiol 70 (8), 975–991.